

Soliton compression and pulse-train generation by use of microchip Q-switched pulses in Bragg gratings

Joe T. Mok, Ian C. M. Littler, Eduard Tsoy, and Benjamin J. Eggleton

ARC Centre of Excellence for Ultrahigh-Bandwidth Devices for Optical Systems, School of Physics,
University of Sydney, Sydney, NSW 2006, Australia

Received March 22, 2005; revised manuscript received April 29, 2005; accepted May 16, 2005

Pulse compression and pulse-train generation are demonstrated by use of kilowatt 580 ps pulses generated by a compact (15 cm × 3 cm × 3 cm) microchip Q-switched laser followed by a fiber Bragg grating. A 12-fold pulse compression to 45 ps with five times peak power enhancement is achieved at 1.4 kW through soliton effect compression in the fiber grating. At 2.5 kW, modulational instability leads to a train of high-contrast sub-100 ps pulses. These demonstrations take advantage of the ultrastrong dispersion at frequencies close to the edge of the photonic bandgap. Experimental results are discussed in the context of the nonlinear Schrödinger equation and are compared with simulations of the nonlinear coupled-mode equations. © 2005 Optical Society of America

OCIS codes: 190.5530, 320.5520, 190.4370.

Photonic crystals are strongly dispersive and can enhance nonlinearities at frequencies close to the edge of the photonic bandgap. These properties provide novel ways to implement miniaturized devices with optical signal processing capabilities. Nonlinear photonic crystals are particularly well suited for achieving efficient optical pulse compression based on soliton-effect compression,¹ which relies on the interplay of dispersion and self-phase modulation. Fiber Bragg gratings (FBGs), as an example of one-dimensional photonic crystals,² offer an ideal geometry for exploring such nonlinear pulse propagation effects, with previous reports of compression of 100 ps pulses generated from a main-frame mode-locked, Q-switched YLF laser.^{3,4}

The ability to compress nanosecond Q-switched pulses is an attractive alternative to mode-locking techniques or to an optical bench sized bulk-optic setup for the generation of sub-50 ps pulses. Whereas commercially available Q-switched lasers can be compact and cost significantly less than main-frame mode-locked lasers, the compression of Q-switched generated pulses is difficult, requiring large dispersion. This means either using a soliton-effect compressor based on an optical fiber that is tens of kilometers long,⁵ which can be lossy, or using bulk grating pairs with impractically large separation (>100 m) in a grating compressor.⁶

In this Letter we demonstrate generation of multi-kilowatt peak power, sub-50 ps pulses by compressing Q-switched laser pulses, using soliton-effect compression in a one-dimensional photonic crystal. We report a 12-fold compression of 580 ps pulses to 45 ps pulses as well as the generation of a train of sub-100 ps pulses by use of a Q-switched YAG laser followed by a 10 cm FBG employed in transmission. These results demonstrate an important practical application of nonlinear photonic crystals for generating intense picosecond pulses from a low-cost, compact (15 cm × 3 cm × 3 cm) Q-switched laser. Experimental results are compared with simulations

and discussed in the context of the nonlinear Schrödinger equation (NLSE).

Nonlinear pulse propagation in a FBG is described by the nonlinear coupled-mode equations (NLCMEs)

$$\frac{i}{V} \frac{\partial A_{\pm}}{\partial t} \pm i \frac{\partial A_{\pm}}{\partial z} + \kappa A_{\mp} + \gamma(|A_{\pm}|^2 + 2|A_{\mp}|^2)A_{\pm} = 0, \quad (1)$$

where A_{\pm} is the pulse envelope of the forward-(backward-) propagating wave, V is the group velocity in the grating's absence, γ is the fiber nonlinearity, and $\kappa \approx \pi \Delta n / \lambda_B$ is the grating coupling coefficient. The amplitude of the index modulation is Δn , and $\lambda_B = 2n_0 \Lambda$ is the Bragg wavelength, where Λ is the grating pitch and n_0 is the mode's effective index.

If the pulse is such that its spectral width $\Delta \omega$ is $\ll c\kappa/n_0$, the NLCMEs can be approximated by the well-known NLSE⁷:

$$\frac{\partial A}{\partial z} + \frac{1}{V_g} \frac{\partial A}{\partial t} + i \frac{\beta_2}{2} \frac{\partial^2 A}{\partial t^2} = iM\gamma|A|^2 A, \quad (2)$$

where A represents the envelope of the entire field⁴ and V_g and β_2 are the group velocity and the group-velocity dispersion inside the grating at the frequency of the field, respectively. $M = [1 + \kappa^2 / (2\delta^2)] / [1 - (\kappa/\delta)^2]$ is a nonlinearity enhancement factor that is due to group-velocity reduction and resonant effects in FBGs.⁴ The detuning of laser wavelength λ from λ_B is $\delta = 2n_0 \pi (\lambda^{-1} - \lambda_B^{-1})$. The dispersion of a FBG in transmission (end effects are ignored) is given by $\beta_2 = -[\text{sgn}(\delta) \kappa^2 n_0^2 / c^2] [\delta^2 - \kappa^2]^{-3/2}$. The NLSE approximation to propagation in gratings provides a framework that borrows from well-known literature for propagation in nonlinear dispersive systems.⁸ For instance, a high-order soliton of the form $A(t) = P_0^{1/2} \text{sech}(t/T_0)$ with peak power P_0 such that $N = (\gamma M P_0 T_0^2 / |\beta_2|)^{1/2} \gg 1$ undergoes pulse narrowing during the initial stage of a soliton period, with the compression factor given by $F_c = 4.1N$ at the optimum length.⁹ At higher

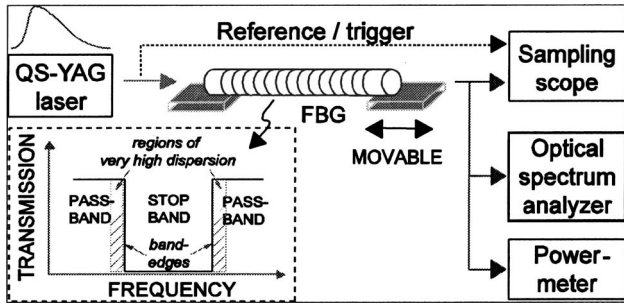


Fig. 1. Experimental setup and illustration of the spectral response of a fiber Bragg grating. QS, Q-switched. Inset, regions of very high dispersion (hatched) are adjacent to the stop band.

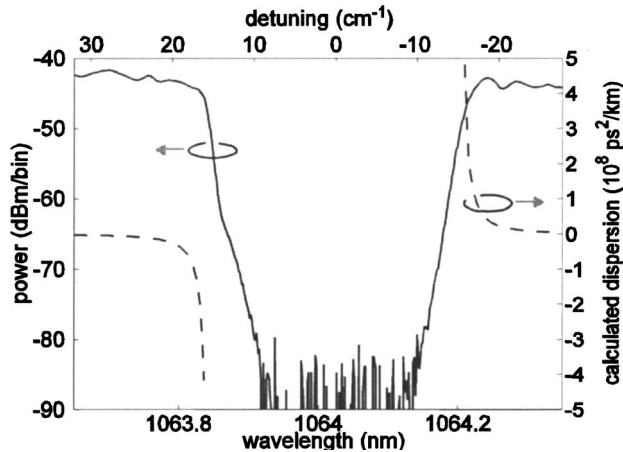


Fig. 2. Measured transmission spectrum (solid curve) and calculated dispersion (dashed curves) of the fiber grating.

launch powers, a periodic pulse train can be generated by modulational instability (MI),⁵ with the periodicity given by $T_{MI} = 2\pi[|\beta_2|/(2M\gamma P_0)]^{1/2}$, where P_0 is the power of the input cw radiation. In the experiment described below, the input pulse is long enough to be considered quasi-cw. With $|\beta_2| \sim 10^8 \text{ ps}^2/\text{km}$, $M \sim 5-10$, and $\gamma \sim 4.3 \text{ W}^{-1} \text{ km}^{-1}$, $N \sim 4.6, 7.5$ at launch peak powers of 1.4 and 2.5 kW, respectively.

The experimental setup (Fig. 1) consists of a Q-switched YAG laser at 1064.34 nm and a 10 cm fiber grating with one end mounted on a translation stage. The grating is enclosed to prevent air currents from causing temperature fluctuations to affect the properties of the FBG. The pulsed source is a JDSU MicroChip NanoPulse Q-switched laser. We estimate the pulse spectral width to be 3–4 pm. The FBG's Bragg wavelength, hence the dispersion at the laser wavelength, is strain tuned by means of the translation stage with a $0.1 \mu\text{m}$ spatial resolution, corresponding to $\sim 0.1 \text{ cm}^{-1}$ in detuning. The FBG, fabricated by use of a photosensitive fiber with the phase-mask technique, is apodized by use of 15% of its total length at each end. The UV-induced loss is 20% in total. The measured transmission spectrum and calculated dispersion of the FBG are shown in Fig. 2, which indicates sidelobe suppression to 1–2 dB, whereas the reflection is well above 40 dB. The photonic bandgap is centered at 1064.0 nm when the grating is unstrained. The 3 dB bandgap width is

0.38 nm, implying that $\kappa = 15.2 \text{ cm}^{-1}$. The output is monitored by use of a sampling oscilloscope with 22 ps overall resolution and an optical spectrum analyzer with 18 pm resolution. We measured the transmitted power with a powermeter to locate the band edge and to estimate the detuning δ .

Figure 3 shows the measured transmission and the output pulse near the short-wavelength band edge at peak power of 1.4 kW. Insets (a)–(e) of Fig. 3 illustrate the output pulse being gradually compressed when it is tuned closer to the band edge. The pulses designated (a) and (e) in Fig. 3 are replotted and compared in Fig. 4. In Fig. 4 (top) the dotted curve represents the output when the band edge is detuned far ($\sim 4.5 \text{ cm}^{-1}$) from the laser wavelength and effectively shows the input pulse. The solid curve represents the measured output at optimum compression, where the estimated detuning is 15.9 cm^{-1} . There is a 12-fold pulse compression from 580 to 45 ps, and a five times peak power enhancement from 580 to 5.4 kW. The

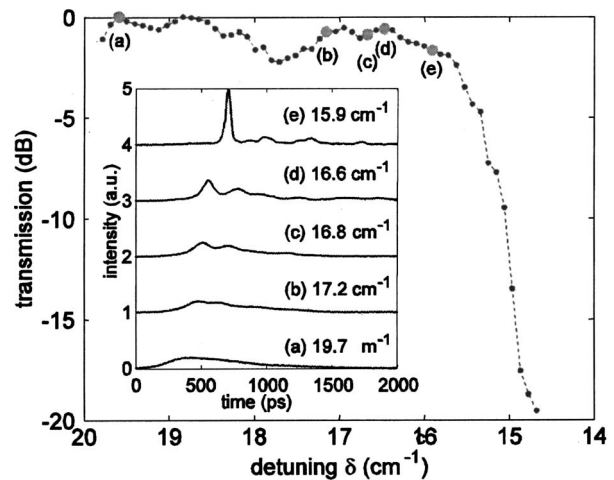


Fig. 3. Measured grating transmission near the short-wavelength band edge at a launch peak power of 1.4 kW. Inset, output pulses at various detunings.

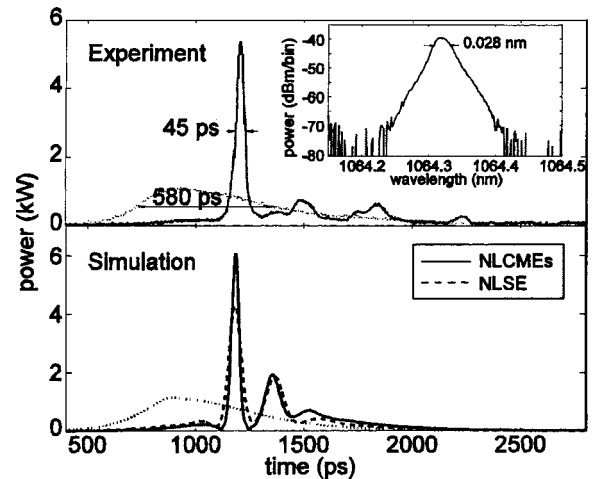


Fig. 4. Twelve-fold pulse compression at a launch peak power of 1.4 kW. Top, measured uncompressed (dotted curve) and compressed (solid curve) pulses. Inset, measured spectrum of the compressed output. Bottom, corresponding simulations at $\delta = 20.0$ (dotted curve, NLCME) and 16.7 cm^{-1} (solid curve, NLCME; dashed curve, NLSE).

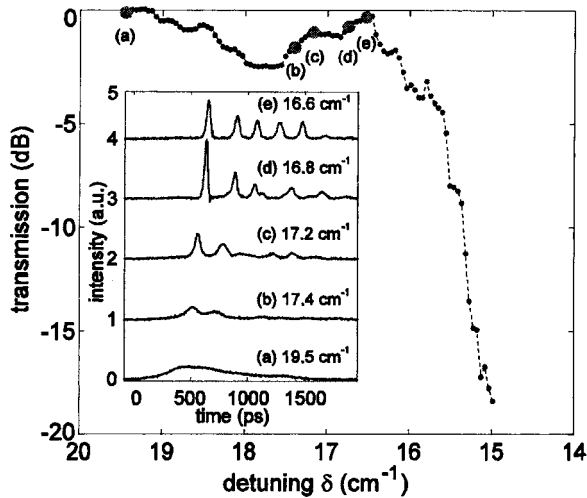


Fig. 5. Measured grating transmission and output pulses (inset) at various detunings at a launch peak power of 2.5 kW.

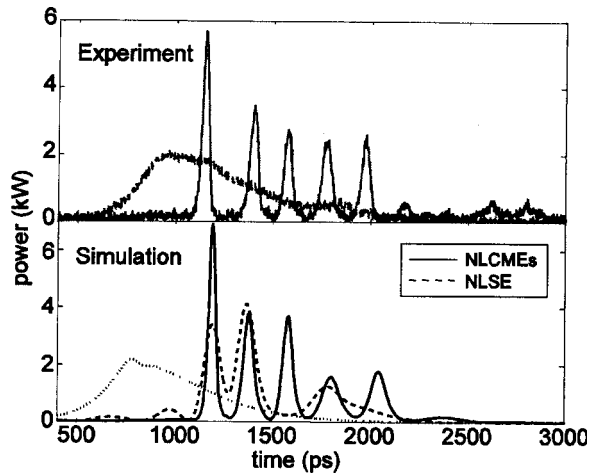


Fig. 6. Generation of a train of sub-100 ps pulses at a launch peak power of 2.5 kW. Top, measured waveforms at $\delta=19.5\text{ cm}^{-1}$ (dotted curve) and 16.6 cm^{-1} (solid curve). Bottom, corresponding simulations at $\delta=20.0$ (dotted curve, NLCME) and 16.0 cm^{-1} (solid curve, NLCME; dashed curve, NLSE).

inset in Fig. 4 shows the measured spectrum of the compressed pulse with a measured 3 dB spectral width of 0.028 nm. Considering only the main pulse and ignoring the pedestal yield a time-bandwidth product of 0.331, which is within 10% of a transform-limited sech^2 pulse. As detuning is inferred from the strain and estimated with respect to the band edge, it is accurate to $0.5\text{--}1.0\text{ cm}^{-1}$.

The soliton order at largest compression is 4.6, which, under the NLSE approximation, gives the expected optimum compression factor F_c of 18.7 and the optimum grating length of 25 mm. Simulated output pulses at $\delta=20.0, 16.7\text{ cm}^{-1}$ calculated by numerical solution of the NLCMEs and then convolved with the detector response are shown in Fig. 4 (bottom). As in the experiment, detuning values are chosen to give the best compression and are slightly different from, but within the uncertainty of, those in the experiment. Although we do not show it here, we observed

both experimentally and numerically that the output pulse shape is highly sensitive to detuning variation (to 0.1 cm^{-1}), because it greatly alters both the dispersive and the nonlinear properties of the FBG. A simulation that uses the NLSE including the third- and fourth-order dispersion terms is also plotted in Fig. 4 (bottom). Both NLCME and NLSE simulations show good agreement with the experiment.

Figure 5 shows the measured transmission and the output pulses at several detunings at a peak power of 2.5 kW. As shown in curve (e) of Fig. 5, a train of short pulses is generated at 16.6 cm^{-1} . Pulses (a) and (e) in the inset of Fig. 5 are compared in Fig. 6 (top), which illustrates that the output consists of five high-contrast pulses with durations from 42 to 60 ps. The pulse separation ranges from 180 to 250 ps. The expected periodicity is 206 ps, which is within the measured values. Shown in Fig. 6 (bottom) are the outputs simulated by use of the NLCMEs and the NLSE at $\delta=20, 16.0\text{ cm}^{-1}$. Whereas NLCMEs produce good agreement with the measured output, the NLSE does not describe pulse propagation within this regime so accurately.

In conclusion, we have demonstrated a 12-fold pulse compression with five times peak power enhancement from a 580 ps pulse at 1.4 kW launch peak power by means of soliton compression in a fiber Bragg grating. At a peak power of 2.5 kW, we observed a breakup of the same input pulse into a series of sub-100 ps pulses under the effect of modulation instability. Simulations that use the NLCMEs show good agreement with experimental results, whereas the theory of modulational instability provides an approximate figure for the periodicity of the output pulse train. The combination of a compact, low-cost microchip Q-switched laser and a 10 cm long fiber Bragg grating offers an alternative source for sub-50 ps pulses.

This research was produced with the assistance of the Australian Research Council (ARC) under the ARC Centres of Excellence program. J. T. Mok's e-mail address is j.mok@physics.usyd.edu.au.

References

1. H. G. Winful, *Appl. Phys. Lett.* **46**, 527 (1985).
2. R. E. Slusher and B. J. Eggleton, *Nonlinear Photonic Crystals* (Academic, 2002).
3. B. J. Eggleton, R. E. Slusher, C. M. de Sterke, P. A. Krug, and J. E. Sipe, *Phys. Rev. Lett.* **76**, 1627 (1996).
4. B. J. Eggleton, C. M. de Sterke, A. B. Aceves, J. E. Sipe, T. A. Strasser, and R. E. Slusher, *Opt. Commun.* **149**, 267 (1998).
5. L. F. Mollenauer, R. H. Stolen, J. P. Gordon, and W. J. Tomlinson, *Opt. Lett.* **8**, 289 (1983).
6. C. V. Shank, R. L. Fork, R. Yen, R. H. Stolen, and W. J. Tomlinson, *Appl. Phys. Lett.* **40**, 761 (1982).
7. B. J. Eggleton, C. M. de Sterke, and R. E. Slusher, *J. Opt. Soc. Am. B* **16**, 587 (1999).
8. G. P. Agrawal, *Nonlinear Fiber Optics* (Academic, 2001).
9. E. M. Dianov, Z. S. Nikonova, A. M. Prokhorov, and V. N. Serkin, *Sov. Tech. Phys. Lett.* **12**, 311 (1986).